

Phase slip and the spatiotemporal response of charge-density waves in NbSe₃

T. L. Adelman, M. C. de Lind van Wijngaarden, S. V. Zaitsev-Zotov,* D. DiCarlo, and R. E. Thorne
 Laboratory of Atomic and Solid State Physics and Materials Science Center, Cornell University, Ithaca, New York 14853
 (Received 10 May 1995)

We have performed spatially resolved measurements of the charge-density-wave (CDW) response to bipolar current pulses. These measurements directly yield the temporal evolution of the CDW elastic force profile and the distribution of CDW phase slip. The steady-state elastic force profile is strongly coupled to the phase-slip distribution. This coupling increases the CDW strain gradient near the current contacts, and reduces the size of the region in which significant phase slip occurs. We describe a model for CDW dynamics in the presence of phase slip that provides an excellent account of the complex spatiotemporal response.

In quasi-one-dimensional metals such as NbSe₃, formation of charge-density waves (CDW's) results in a host of interesting transport effects.¹ A CDW consists of a lattice distortion coupled to an electron density modulation $\Delta n(x) = n_1 \cos[Qx + \phi(x,t)]$, where $Q = 2k_F$ is the CDW wave vector and ϕ is the phase of the CDW order parameter. In the presence of impurities, the CDW becomes pinned through spatial variations of ϕ . For electric fields greater than a threshold field E_T , the CDW can depin from the impurities and slide through the crystal, resulting in spatial and temporal fluctuations of ϕ and a collective current $i_c \propto \partial\phi/\partial t$.

When CDW motion is induced between current contacts (as in Fig. 1), the CDW well beyond the contacts must remain pinned. The CDW thus compresses near one contact and stretches near the other, resulting in a macroscopic spatial variation of ϕ and a strain $\epsilon_x \propto \partial\phi/\partial x$.²⁻⁵ As in superconductors, these phase gradients lower the barrier for phase slip via formation of CDW dislocations, allowing conversion between CDW current and single-particle current near the contacts.^{2-4,6-9} The net phase slip rate is determined by the strain profile, and determines the steady-state CDW current. Transport measurements^{3,10-12} are consistent with some features of a model⁷ for thermal nucleation of dislocation loops in the presence of a linear strain profile, and x-ray scattering measurements¹³ have provided direct evidence for the CDW strains which drive phase slip.

CDW phase slip is of interest both as a fundamental CDW process and as a prototype for analogous phenomena in superconducting, superfluid, and pattern-forming systems. Here we describe spatially resolved measurements of the CDW response to bipolar current pulses. These measurements probe the local CDW elastic force, and directly yield

the spatial distribution of phase slip and the temporal evolution of the CDW strain profile. While previous work has shown that the strain profile determines the net phase slip rate, we show that the distribution of phase slip strongly affects the strain profile.¹⁴ We describe a simple model for CDW motion in the presence of phase slip that accounts quantitatively for many features of the measured response. These results have important implications for our understanding of CDW transport.

High-purity NbSe₃ single crystals were held to alumina substrates patterned with an array of 2- μm -wide, 0.25- μm -high contacts (shown in Fig. 1) using a thin polymer film. Typical contact resistances were 300 Ω , roughly two orders of magnitude larger than the sample resistance between contacts. Combined with NbSe₃'s electronic anisotropy, these resistances ensured that the contacts were essentially nonperturbing.

Current pulses of alternating sign were applied to the current contacts, and the response was measured for each adjacent pair of voltage contacts. The total applied current i_{tot} flows as single-particle and CDW currents, $i_{\text{tot}}(t) = i_s(x,t) + i_c(x,t)$. CDW motion thus reduces the single-particle current below i_{tot} and changes the sample voltage by

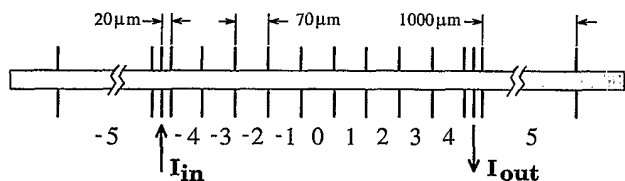


FIG. 1. Contact geometry used in the experiments. Numbers refer to sample segments between adjacent contacts.

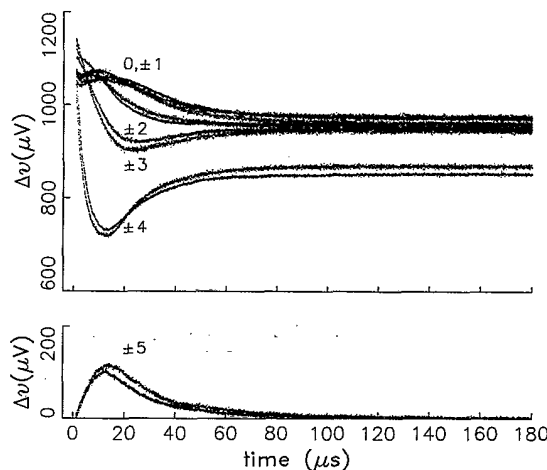


FIG. 2. CDW response in NbSe₃ at $T=90$ K to a sign reversal of an applied current $|i_{\text{tot}}| \approx 5I_T$, for each of the sample segments in Fig. 1.

$$\Delta v = \int \rho_s i_c(x, t) dx, \quad (1)$$

where ρ_s is the single-particle resistance per unit length, and the integral is taken between the voltage contacts. As first observed by Gill,^{2,3} the voltage immediately after a reversal of the current direction is smaller than its steady-state value, indicating that there is a transient excess CDW current. Gill suggested³ that the transient is due to CDW motion between the steady-state strained profiles appropriate to the two current directions.

Figure 2 shows the CDW response (Δv) to a current sign reversal with $|i_{\text{tot}}| \approx 5I_T$ (where I_T is the threshold current corresponding to E_T) for each of the sample segments indicated in Fig. 1. The response is symmetric about the midpoint between the current contacts, and has faster initial time scales and larger transients near the current contacts. Unlike the response measured for widely separated voltage contacts,^{2,3} the response of the segments is nonmonotonic, especially near the current contacts. Transient CDW motion is also observed beyond the current contacts.¹⁵ The steady-state CDW current is largest in the middle of the sample and decreases as the current contacts are approached, indicating that phase slip occurs at significant distances from the current contacts.¹⁶

To interpret our measurements we begin by considering a simplified, one-dimensional version of the Fukuyama-Lee-Rice model,¹⁷

$$\gamma \frac{\partial \phi}{\partial t} = \left(\frac{en_c}{Q} \right) (E - E_P) + K \frac{\partial^2 \phi}{\partial x^2}, \quad (2)$$

where γ is the CDW damping constant, n_c is the CDW condensate density, K is the CDW elastic constant, E is the applied electric field, and where the effects of CDW interaction with impurities are accounted for by a phenomenological pinning field E_P , taken to be a function of i_c . The measurements fix the total current i_{tot} rather than the electric field E . Using $E = \rho_s i_s$ and $\gamma = (en_c/Q)^2 A \rho_c$, Eq. (2) can be rewritten as

$$i_c = \frac{1}{\rho_c + \rho_s} \left[\rho_s i_{\text{tot}} - E_P + \left(\frac{en_c}{Q} \right)^{-1} K \frac{\partial^2 \phi}{\partial x^2} \right], \quad (3)$$

where ρ_c is the high-field CDW resistance per unit length, $i_c = A(en_c/Q)\partial\phi/\partial t$, and A is the crystal cross-sectional area.

The variation of E_P with CDW current magnitude is very weak (except very near threshold), and the time scale of its change in sign in response to changes in current direction is much shorter than can be resolved in our measurements.¹⁸ The transient variation of i_c is thus due only to $K\phi''$. Consequently, the position-dependent pulse response in Fig. 2 provides the temporal evolution of the CDW elastic force profile.

The coupling between $i_c(x, t)$ and $K\phi''(x, t)$ implied by Eq. (3) can be directly tested in the steady state. The steady-state response in Fig. 2 gives $i_c(x, t \rightarrow \infty)$. The steady-state response obtained when i_{tot} is injected through the outermost contact pair in Fig. 1 gives $i_c^0(i_{\text{tot}}) \equiv [1/(\rho_c + \rho_s)](\rho_s i_{\text{tot}}$

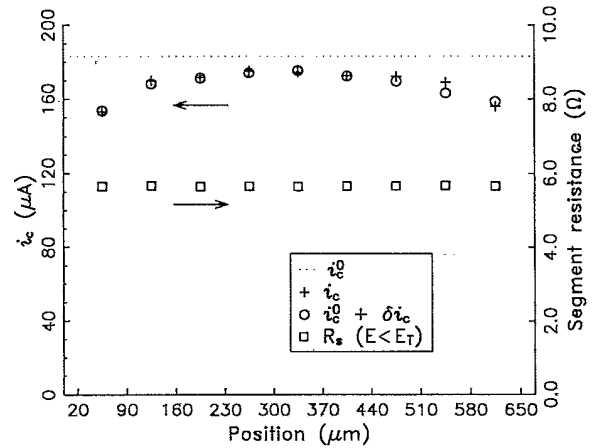


FIG. 3. Comparison of measured values of i_c and $i_c^0 + \delta i_c$. Current contacts are located at positions corresponding to the left and right vertical axes. The single-particle resistance $R_s = v/i_{\text{tot}}$ measured with $E < E_T$ is the same for all segments and is independent of sample history, indicating that the decrease of $i_c(x)$ near the current contacts is not due to contact-geometry-related field variations or to modulation of R_s by CDW deformations.

$-E_P)$, since $K\phi''$ is small for large contact separations.¹⁹ The difference between the initial transient and steady-state responses,

$$\delta i_c(i_{\text{tot}}) = [i_c(x, t \rightarrow \infty) - i_c(x, t = 0^+)]/2,$$

gives

$$\delta i_c(i_{\text{tot}}) \equiv \frac{1}{\rho_c + \rho_s} \left(\frac{en_c}{Q} \right)^{-1} K \phi''(x, t \rightarrow \infty).$$

In the steady state the elastic force hinders CDW motion between the current contacts; when the driving current i_{tot} changes sign, the elastic force initially aids CDW motion by an amount equal to its hindrance in the steady state. Equation (3) thus predicts a quantitative connection between the dc and transient CDW current profiles, $i_c(x, t \rightarrow \infty) = i_c^0 + \delta i_c$.

Figure 3 compares measured values of $i_c(x, t \rightarrow \infty)$ and $i_c^0 + \delta i_c$. The excellent agreement (with no adjustable parameters) confirms the coupling between the CDW current and the elastic force. Furthermore, Fig. 3 indicates that phase slip—which produces the conversion between i_c and i_s near the current contacts—has a dramatic effect on the elastic force profile. For example, at 55 μm from the current contacts i_c is only 10% below its mid-sample value, but this increases the elastic force [measured down from i_c^0 to $i_c(x, t \rightarrow \infty)$] by more than a factor of 3.

Because of this strong coupling between phase slip and the elastic force, phase slip must be included in calculating the transient response of Fig. 2.¹⁴ Consistent with previous work,⁷ we assume phase slip occurs at a strain-dependent rate,

$$r_{\text{ps}} = r_0 \exp \left[- \left| \left(\frac{en_c}{Q} \right) \frac{V_a}{2K(\partial\phi/\partial t)} \right| \right], \quad (4)$$

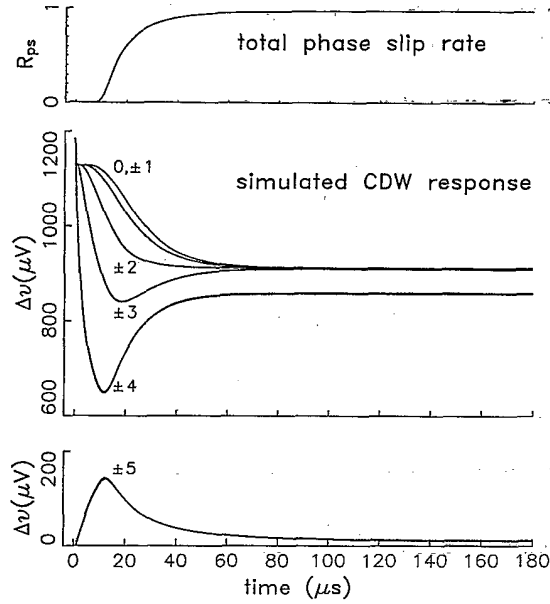


FIG. 4. CDW response to a sign reversal of the applied current calculated using Eq. (5), for the contact configuration in Fig. 1. $R_{ps}(t)$ is the total phase-slip rate $\int_{-\infty}^{+\infty} |r_{ps}| dx$ normalized by its steady-state value.

where V_a and r_0 are related to the barrier height and attempt rate for dislocation loop nucleation, respectively. Since the CDW phase in the presence of phase slip is no longer well defined, we solve instead for a “renumbered” phase variable $\theta(x, t)$ determined by

$$\frac{\partial \theta}{\partial t} = \frac{1}{A} \left(\frac{en_c}{Q} \right)^{-1} \tilde{i}_c[i_{tot}, \theta(x, t)] - \int_{-\infty}^x r_{ps}[\theta(x', t)] dx', \quad (5)$$

where $\tilde{i}_c[i_{tot}, \theta(x, t)]$ is the solution of Eq. (3) using the elastic force profile determined by $\theta''(x, t)$, the experimentally measured $E_P(i_c)$, and the applied current i_{tot} . \tilde{i}_c calculated in this way corresponds to the CDW current measured by Δv . The renumbering of the phase due to phase slip is given by $\int_{-\infty}^x r_{ps}[\theta(x', t)] dx'$.

Figure 4 shows the response calculated using Eq. (5) for a driving current equal to that of Fig. 2 assuming $V_a = 35$ mV, $K = 9.1 \times 10^{-3}$ eV \AA^{-2} , and $r_0 = 3 \times 10^{15}$ s $^{-1}$ m $^{-1}$, roughly consistent with previously reported values.^{10,13,20}

Figure 5(a) shows the predicted temporal evolution of the CDW strain profile corresponding to the response of Fig. 4. As discussed above, the measured transient response $\Delta v \propto i_c$ gives the elastic force $K\phi''$. Thus, the strain at each of the contacts can be determined from Δv and the measured dc I - V characteristic i_c^0 as

$$\begin{aligned} \varepsilon_x(x_c, t) &= \int_0^{x_c} K\phi''(x, t) dx \\ &= \frac{(\rho_c + \rho_s)}{\rho_s} \left(\frac{en_c}{Q} \right) \left(\sum_n \Delta v_n - x_c \rho_s i_c^0 \right), \end{aligned}$$

where x_c is the position of the contact and the sum is over the response v_n for contact pairs located between $x=0$ and $x=x_c$. Note that this gives the exact strain at each contact,

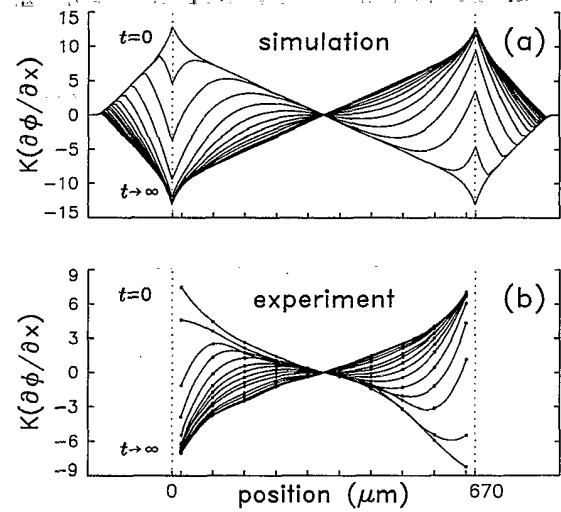


FIG. 5. (a) Calculated and (b) measured CDW strain profiles in response to a current sign reversal, in units of $\mu\text{eV} \text{\AA}^{-2}$, at $t=0, 1, 5, 10, 15, 20, \dots, 190$ μs . Current contact positions are indicated by the dotted vertical lines. The measured strain is determined only at the voltage contact positions (indicated by dots); the solid lines are guides to the eye.

not a spatial average. Figure 5(b) shows the resulting time-dependent strain profile. The correspondence between the calculated and measured profiles is very good.

The model thus reproduces most of the important qualitative features seen in Figs. 2 and 5(b), and provides insight into their origin. Just before the applied current changes sign, the elastic force opposing CDW motion is largest near the current contacts (segments ± 4), where phase slip produces a smaller steady-state CDW current. Just after the sign change, the elastic force aids CDW motion, and thus drives a larger transient CDW current (proportional to Δv in Fig. 2) near the current contacts. This motion is quickly held back by the section of the CDW beyond the current contacts (segments ± 5), leading to a rapid decay of the CDW current and to an increase in strain near the contacts. As the strain near the contacts builds, it eventually becomes large enough to induce significant phase slip. Phase slip increases the CDW current from its minimum at the “dip” towards a larger steady-state value, and limits subsequent growth of the strain near the contacts. Since CDW motion beyond the current contacts (segments ± 5) is only driven by this strain, the dips observed just inside the current contacts (segments ± 4) nearly coincide with the peaks observed just outside (segments ± 5). Near the middle of the sample (segments 0, ± 1), the CDW moves independent of the region beyond the contacts for a longer time, producing a slower transient. The response here is monotonic, since phase slip is already occurring by the time the middle region’s elastic force changes sign.

The most significant discrepancy between the calculations and experiment is in the distribution of phase slip. In the calculations essentially no slip occurs at distances greater than 90 μm , whereas in the experiment roughly 4% of the slip occurs there. The origin of this discrepancy is unclear.

Finally, we emphasize a few important results of the present work.

(1) Phase slip strongly affects the transient CDW response, especially near the current contacts.

(2) The phase-slip-related decrease of CDW current near the current contacts enhances the CDW strain gradient there, producing a nonlinear strain profile.

(3) The enhanced CDW strain gradient reduces the distance from the current contacts at which significant phase slip occurs. Assuming a linear slip profile between the current contact and segment 4, we estimate that at least half of the slip in our experiment occurs less than 25 μm from the current contact.

(4) The coupling between phase slip and CDW strain has important consequences for many aspects of CDW transport,²¹ including the form of the CDW current-phase-slip voltage relation;^{3,7,9-12} the interpretation of the phase-slip voltage; the form of the CDW current-voltage characteristic near threshold; the transient and large-signal ac responses; and the voltage and temperature dependences of coherent oscillations and Shapiro steps.¹

(5) The transient evolution of CDW deformations extending beyond the current contacts affects the response between the contacts. Nearly one-third of the mid-sample phase displacement under the conditions studied here is due to deformations beyond the contacts.

(6) Previous analysis^{3,22} of the CDW response to bipolar current pulses equated the charge $\Delta\bar{q} = \int_0^\infty [i_c(t) - i_c(t \rightarrow \infty)] dt$ with the CDW displacement between steady-state configurations of opposite deformation. This charge and displacement are not equivalent because the total CDW current is a mix of polarization and phase-slip currents, and the polarization current is significantly larger than the transient excess during most of the transient. From our simulation with conditions as in Fig. 5, the CDW displacement between current contacts is a factor of 10 larger than that corresponding to the charge $\Delta\bar{q}$.

We wish to acknowledge fruitful conversations with V. Ambegaokar. Substrates were prepared at the National Nanofabrication Facility at Cornell University. This work was supported by NSF Grant No. DMR92-04169.

*Permanent address: Institute of Radioengineering and Electronics, Russian Academy of Sciences, Moscow, Russia.

¹For comprehensive reviews of CDW's, see P. Monceau, in *Electronic Properties of Quasi-One-Dimensional Materials*, edited by P. Monceau (Reidel, Dordrecht, 1985), Pt. II, p. 139; G. Grüner, *Rev. Mod. Phys.* **60**, 1129 (1988).

²J. C. Gill, *Solid State Commun.* **44**, 1041 (1982).

³J. C. Gill, *J. Phys. C* **19**, 6589 (1986).

⁴D. Feinberg and J. Freidel, in *Low-Dimensional Electronic Properties of Molybdenum Bronzes and Oxides*, edited by C. Schlenker (Kluwer Academic, Dordrecht, 1989), p. 407.

⁵S. E. Brown, L. Mihaly, and G. Grüner, *Solid State Commun.* **58**, 231 (1986).

⁶K. Maki, *Physica B+C* **143B**, 59 (1986).

⁷S. Ramakrishna, M. P. Maher, V. Ambegaokar, and U. Eckern, *Phys. Rev. Lett.* **68**, 2066 (1992).

⁸N. P. Ong, G. Verma, and K. Maki, *Phys. Rev. Lett.* **52**, 663 (1984); L. P. Gor'kov, *Pis'ma Zh. Eksp. Teor. Fiz.* **38**, 76 (1983) [*JETP Lett.* **38**, 87 (1983)].

⁹For a comprehensive review of previous work on CDW phase slip, see F. Ya. Nad', in *Charge Density Waves in Solids*, edited by L. P. Gor'kov and G. Grüner (Elsevier, New York, 1989), p. 189.

¹⁰M. P. Maher, T. L. Adelman, S. Ramakrishna, J. P. McCarten, D. A. DiCarlo, and R. E. Thorne, *Phys. Rev. Lett.* **68**, 3084 (1992); M. P. Maher *et al.* (unpublished).

¹¹P. Monceau, M. Renard, J. Richard, and M. C. Saint-Lager, *Physica B+C* **143B**, 64 (1986).

¹²D. V. Borodin, S. V. Zaitsev-Zotov, and F. Ya. Nad', *Zh. Eksp. Teor. Fiz.* **93**, 1394 (1987) [*Sov. Phys. JETP* **66**, 793 (1987)].

¹³D. DiCarlo, E. Sweetland, M. Sutton, J. D. Brock, and R. E. Thorne, *Phys. Rev. Lett.* **70**, 845 (1993); E. Sweetland, A. C.

Finnefrock, W. J. Padulka, M. Sutton, J. D. Brock, D. DiCarlo, and R. E. Thorne, *Phys. Rev. B* **50**, 8157 (1994).

¹⁴J. C. Gill [in *Charge Density Waves in Solids*, edited by Gy. Hutiray and J. Solyom (Springer, Berlin, 1985), p. 377] noted that phase slip would limit the maximum CDW strain.

¹⁵M. C. Saint-Lager, P. Monceau, and M. Renard [*Synth. Met.* **29**, F279 (1989)] observed evidence for CDW deformations beyond current contacts in dc measurements.

¹⁶J. C. Gill [*Phys. Rev. Lett.* **70**, 331 (1993)] and M. E. Itkis and S. V. Zaitsev-Zotov [*J. Phys. (Paris) IV* **2**, 193 (1993)] attempted to measure the phase slip profile in NbSe₃, but contact perturbations and contact quality problems made interpretation of their results difficult.

¹⁷H. Fukuyama and P. A. Lee, *Phys. Rev. B* **17**, 535 (1978); P. A. Lee and T. M. Rice, *ibid.* **19**, 3970 (1979).

¹⁸For the segment-to-segment distribution of steady-state i_c values in Fig. 2, $E_p(i_c)$ determined from the measured dc I - V responses varies by only 1%, and this produces only a 0.1% variation in $\rho_s i_{\text{tot}} - E_p$. The time scale of E_p 's response can be determined at $T=120$ K, where CDW deformations due to boundary conditions are very small.

¹⁹The CDW strain ϕ' near the current contacts determines the slip rate and CDW current, and for a given current is essentially independent of current contact separation (Refs. 3, 4, and 10). The strain gradient $K\phi''$ is thus small for large contact separations.

²⁰Previous experimental estimates of K , V_a , and r_0 assumed that the CDW strain profile was linear, contrary to the present results.

²¹T. L. Adelman *et al.* (unpublished).

²²M. E. Itkis and J. W. Brill, *Phys. Rev. Lett.* **72**, 2049 (1994); J. Zhang, J. F. Ma, S. E. Nagler, and S. E. Brown, *ibid.* **70**, 3095 (1993); Z. Z. Wang and N. P. Ong, *ibid.* **58**, 2375 (1987).